Brain Structure and Function
https://doi.org/10.1007/s00429-020-02128-0

ORIGINAL ARTICLE

Dissociable fronto-striatal functional networks predict choice impulsivity

Qiang Wang[1,2,3] · Chenyu Lv[4] · Qinghua He[4,5] · Gui Xue[6]

Received: 18 November 2019 / Accepted: 7 August 2020

Abstract

Fronto-striatal structural connectivity is associated with choice impulsivity. Yet, to date, whether distinct fronto-striatal functional coupling associates with impulsive choices are largely unknown. Using seed-based resting-state functional MRI (rsfMRI) combined with multivariate pattern analysis (MVPA), the present study aimed to explore the predictions of dissociable frontal–striatal functional connectivity on choice impulsivity in a relatively large sample ($N = 429$). Adaptive delay-discounting task was utilized to assess choice impulsivity and the striatum was further divided into three subregions including the nucleus accumbens (NAcc), caudate, and putamen. Results revealed that both the functional coupling between the NAcc and the limbic/dorsolateral prefrontal cortex, and between the caudate and the dorsal prefrontal cortex, including the dorsomedial prefrontal cortex (DMPFC), successfully predicted the delay-discounting rate. However, such pattern was not observed in the putamen-prefrontal functional connectivity. These findings suggest fronto-striatal-dependent neural mechanisms of choice impulsivity and further provide a better understanding of the contributions of striatum subregions and their functional connectivities with different areas of prefrontal cortex upon inter-temporal choice.

Keywords Inter-temporal choice · Multivariate pattern analysis · Prefrontal cortex · Choice impulsivity · Striatum · Functional connectivity

Introduction

Impulsivity refers to the tendency to engage in behavior that involves rashness, a lack of foresight or planning, or as behavior that occurs without reflection or careful deliberation (Dawe et al. 2004). As one of the most important sub-component of impulsivity, choice impulsivity exists ubiquitously in our everyday life and preschool children who exhibit low choice impulsivity are more prone to develop into cognitively and socially competent adolescents, manifesting higher scholastic performance and extraordinary ability to coping with frustration and stress (Mischel et al. 1989). In general, the delay-discounting task is behaviorally and objectively utilized to assess and measure impulsivity especially impulsive choice in the laboratory environment (Bari

Electronic supplementary material The online version of this article (https://doi.org/10.1007/s00429-020-02128-0) contains supplementary material, which is available to authorized users.

✉ Qiang Wang
wangqiang113@gmail.com

✉ Qinghua He
heqinghua@swu.edu.cn

✉ Gui Xue
gxue@bnu.edu.cn

[1] Key Research Base of Humanities and Social Sciences of the Ministry of Education, Academy of Psychology and Behavior, Tianjin Normal University, Tianjin 300387, China

[2] Faculty of Psychology, Tianjin Normal University, Tianjin 300387, China

[3] Tianjin Social Science Laboratory of Students' Mental Development and Learning, Tianjin 300387, China

[4] Faculty of Psychology, Southwest University, Chongqing 400715, China

[5] CAS Key Laboratory of Mental Health, Institute of Psychology, Beijing 100101, China

[6] National Key Laboratory of Cognitive Neuroscience and Learning and IDG/McGovern Institute for Brain Research, Beijing Normal University, Beijing 100875, China

Published online: 19 August 2020

and Robbins 2013; Dalley et al. 2011). In this task, individuals are required to choose between a small but immediate benefit and a large but delayed profit. A comparatively high percentage of immediate reward choice rather than delayed reward serves as a promising biomarker for various psychiatric disorders such as substance abuse (Hu et al. 2015; Bickel et al. 1999), pathological gambling (Alessi and Petry 2003), and ADHD (Paloyelis et al. 2010). However, it is still elusive about the precise neurobiological underpinnings of choice impulsivity especially from the perspective of individual differences in a large sample.

Basal ganglia have been implicated in a wide range of functions, including motor, cognitive, motivational, and reward processes (Di Martino et al. 2008). The striatum is a critical component of basal ganglia, and its subdivisions (i.e., the nucleus accumbens [NAcc], caudate, and putamen) exert different involvements of mental processes above-mentioned in impulsivity (Haber and Knutson 2010). In particular, the ventral portion of the striatum (i.e., NAcc) is predominantly involved in the motivation/reward-related processes such as the delayed rewards valuation (Kable and Glimcher 2007; Li et al. 2013), summed value encoding (Cai et al. 2011), and immediate option preference processing (McClure et al. 2004, 2007). Moreover, the ventral striatal activity in response to positive and negative feedback as well as functional connectivity intensity in this region can predict individual's impulsive choice (Hariri et al. 2006; Li et al. 2013). Such prediction likewise is consistently observed even in the absence of choices about future rewards (Cooper et al. 2013). In contrast, the dorsal portion of the striatum (i.e., caudate and putamen) is selectively involved in time and costs estimation for delay-related reward, which perhaps reflects higher-level cognitive processes (Wittmann et al. 2007). Additionally, the dorsal striatum is thought to encode the temporally discounted value difference of the two alternative options (Cai et al. 2011) and be more activated during impulsive choices involving losses (Xu et al. 2009), which also emphasizes the involvement of dorsal striatum on reward-related processes. Taken together, above-mentioned studies suggest that it is a critical step to independently examine striatal subdivisions functions (i.e., cognitive, reward, and motor processing), especially from the perspective of functional connectivity with other brain regions, on choice impulsivity, which will further deeper our understanding of cognitive and neural mechanisms of impulsivity.

Human prefrontal cortex (PFC) is functionally organized as the medial–lateral axis (O'Reilly 2010). The medial areas, especially ventromedial PFC (VMPFC), is preferentially involved in value computation processes (Bechara et al. 2000), such as the delayed reward valuation (Kable and Glimcher 2007; Hare et al. 2014), decision value encoding (Chib et al. 2009), and choice preference processes (McClure et al. 2004). Furthermore, it also links to the representation of recent and distant time information (Koritzky et al. 2013) and cognitive control functions (Ridderinkhof et al. 2004). Similarly, the dorsomedial prefrontal cortex (DMPFC) represents immediate and delayed reward magnitude along the anterior–posterior gradient in choice impulsivity (Wang et al. 2014). Moreover, its morphological characteristics and functional organizations, such as grey matter volume (Wang et al. 2016), regional homogeneity (Lv et al. 2019), and activation patterns during risky decision task (Lv et al. 2020), were found to successfully predict individual's choice impulsivity. These findings support both ventral and dorsal portions of MPFC are crucial for better understanding of choice impulsivity. In contrast, the lateral areas, especially dorsolateral prefrontal cortex (DLPFC), is predominantly engaged in cognitive control processes (Miller and Cohen 2001). In general, this region reflects the ability of top-down cognitive control necessary to resist temptation deriving from immediate reward (Figner et al. 2010; McClure et al. 2004) and represents future reward delay during intertemporal choice (Ballard and Knutson 2009), as well as modulate the computation of stimulus value subserved by VMPFC to choose delayed rewards (Hare et al. 2014). More importantly, the medial and dorsal areas interactions with subcortical brain regions (i.e., striatum) are commonly found to determine the level of choice impulsivity (Peters and Büchel 2011). However, few studies have systematically and independently examine the extent to which different fronto-striatal circuitries support individual's variability in choice impulsivity.

Converging evidence has widely implicated that the striatum receives the structural projections from prefrontal cortex, and that together they underlie distinct psychological processes such as reward-related/motivational processes (i.e., NAcc), executive/cognitive control processes (i.e., caudate), and motor-related processes (i.e., putamen)(Alexander et al. 1986). Such fronto-striatal structural connectivity has been found associated with choice impulsivity. In particular, prior research has emphasized the importance of the cortico-striatal white matter integrity (e.g., caudate and putamen) on choice impulsivity (Peper et al. 2012). Recent research reported that the white matter connectivity estimated by probabilistic tractography of diffusion imaging data between the NAcc and vmPFC/DLPFC, as well as between dorsal striatum and DLPFC, were positively correlated with choice impulsivity (Hampton et al. 2017). Additionally, some studies delineated an opposite associations between the fronto-striatal connectivity and choice impulsivity, that is, greater medial striatum-right DLPFC tract strength correlated with less choice impulsivity (van den Bos et al. 2014, 2015). Moreover, resting-state functional connectivity studies have demonstrated dissociable neural circuits associated with each of striatal subdivisions that are involved into motor, cognitive control, and reward-related processes (Di Martino

et al. 2008), which also highlights the importance of independently examining the different striatal subregions functional loops on choice impulsivity. Based on aforementioned findings concerning on the functions of the subdivisions of striatum and prefrontal cortex upon choice impulsivity, it has been proposed that cognitive control processes subserved by DLPFC selectively enable to modulate the valuation computation subserved by the NAcc via biasing attention away from immediate reward and/or highlighting long-term goals (Figner et al. 2010; Hare et al. 2009) to reduce choice impulsivity. Oversensitivity to immediate reward in valuation networks including NAcc and vmPFC, is believed to be another potential mechanism underlying choice impulsivity (Peters and Büchel 2011; McClure et al. 2004). However, to date, how dissociable fronto-striatal functional connectivities predict choice impulsivity is still largely unclear.

In the present study, we hypothesized that dissociable fronto-striatal functional connectivities could predict choice impulsivity. Specifically, the functional connectivity between (1) the NAcc and vmPFC including orbitofrontal cortex (OFC) and/or dlPFC, (2) the caudate and DLPFC, as well as (3) the putamen and motor cortex might all predict individual's impulsivity. To address these hypotheses, the striatum was divided into three subregions, including the NAcc, caudate, and putamen based on the Harvard–Oxford Structural Atlas, a validated probabilistic atlas included in FSL. After which, a seed-based resting-state functional connectivity analysis was employed to predict individual's choice impulsivity due to that impulsivity has been considered as a stable trait. Compared to univariate analysis, multivariate pattern analysis is considered as a more sensitive tool to uncover the underlying mechanisms how the human brain works and thus was utilized to investigate the association between the fronto-striatal functional couplings and choice impulsivity in a large sample size ($n = 429$).

Materials and methods

Participants

This study was approved by the Institutional Review Board of Southwest University. Written informed consent was obtained from each adult participant (age 18–26) before formal experiments. Four adolescent participants (age 17) were required to sign the consent form after receiving the verbal consent from their parents via telephone.

Four hundred and twenty-nine (315 females and 114 males) healthy Chinese college students were included in the present study (age ranges from 17–26 years old with mean age = 19.58 ± 1.59 years). Subjects were included if they had small head motion during fMRI scans (mean frame-wise displacement [FD] < 1 mm), and good model-fitted behavioral scores (k) based on maximizing the likelihood of the observed choices and visual inspection of fitting curve (van den Bos et al. 2014; Wang et al. 2016). All subjects had no history of psychiatric or neurological disease according to self-report.

Behavioral measures

Adaptive delay-discounting task

The adaptive delay-discounting task was employed to assess impulsive magnitude (Wang et al. 2016; van den Bos et al. 2014). In this task, subjects were required to make a decision between a fixed immediate reward option (SS)(RMB 60) and a varied delayed reward option (LL) (RMB 78–108, to be paid in 15–45 days). Following our previous studies (Wang et al. 2014), the hyperbolic function ($SV = A/(1 + k \times D)$) was used to fit temporal discounting, where SV is the subjective value, A is the reward magnitude, D is the delay time, and k is the delay discounting rate. The initial discounting rate was set to 0.02 and was increased or decreased as a function of participant's choices. Specifically, if the subjects chose the SS option, the delay-discounting rate k was increased by having a larger LL on the next trial. In contrast, if the subjects chose the delay option, the delay discounting rate k was decreased by having a small LL on the next trial. For the first twenty of the total 60 trials, the size of each step was 0.01 and for the remaining 40 trials the step size was 5%. Based on previous findings (Johnson and Bickel 2002; Lagorio and Madden 2005), hypothetical money was served as a valid proxy for real money. In addition, all participants received monetary compensation of RMB 500 at the end of our Gene-Brain-Behavior (GBB) project (Lv et al. 2019, 2020; Wang et al. 2016).

Behavioral data analysis

MATLAB (MathWorks, Natick, MA, USA) was used to perform statistical analyses of the behavioral data. In delay-discounting task, we employed the multidimensional unconstrained nonlinear minimization function (fminsearch) of the optimization toolbox implemented in MATLAB for model fitting. Hyperbolic function ($SV = A/(1 + k \times D)$) was used to compute the subjective value. To model trial-by-trial choice, we utilized a softmax function to calculate the probability of choosing the immediate option (P_{SS}) on trial t as a function of the difference in V_{SS} and V_{LL}: $P_{SS} = 1/(1 + \exp(-1*m*(V_{SS} - V_{LL})))$, where m is the decision slope, V_{SS} and V_{LL} is the subjective value of immediate and delayed option, respectively. Individual discounting rates were determined as the value k that maximized the likelihood of the observed choices. We used log-transformed k

to represent impulsive choice (log$k$) based on prior studies (Van Den Bos et al. 2015; Wang et al. 2016).

Brain imaging data acquisition

All structural and resting-state functional MRI images were acquired on a Siemens 3 T Trio scanner (Siemens Medical Systems, Erlangen, Germany). One session of high-resolution T1-weighted structural images were acquired by using a Magnetization Prepared Rapid Acquisition Gradient-Echo (MPRAGE) sequence: TR/TE = 1900 ms/2.52 ms; inversion time (TI) = 900 ms; Flip angle = 9°; FOV = 256 × 256 mm^2; Slice = 176; thickness = 1.0 mm; voxel size = 1 × 1 × 1 mm^3. Resting state functional MRI images were collected based on the Gradient Echo type Echo Planar Imaging (GRE-EPI) sequence; TR/TE = 2000 ms/30 ms; Flip angle = 90°; Resolution matrix = 64 × 64; FOV = 220 × 220 mm^2; Thickness = 3 mm; slip gap = 1 mm; acquisition voxel size = 3.4 × 3.4 × 4 mm^3. A total of 32 slices were acquired to cover the whole brain. The resting state fMRI images contained 242 volumes with a running time of 8 min 4 s. During the resting-state scanning, all subjects were required to relax and keep their eyes closed but not to sleep (Damoiseaux et al. 2006).

Resting-state fMRI preprocessing

The resting-state fMRI data were preprocessed using Data Processing Assistant for Resting-State fMRI (DPARSF, https://resting-fmri.sourceforge.net/) implemented in the MATLAB (Math works, Natick, MA, USA) platform. The first 10 volumes of each participant were discarded due to the magnetization disequilibrium and the subject's adaptation to the scanning noise. The remaining 232 volumes were slice-timing corrected and then realigned to the middle slice of the brain to correct for head motion. All realigned images were spatially normalized to the MNI template, resample into 3 × 3 × 3 mm^3 resolution, and then smoothed with an isotropic 8 mm FWHM Gaussian kernel. White matter, cerebrospinal fluid, global signal, and six motion parameters for head movement were regressed out as nuisance variables to reduce the effects of head motion and non-neuronal BOLD fluctuations (Fox et al. 2005). Temporal filtering (0.01–0.08 Hz) and voxel-wise linear detrending were also applied to the resting-sate fMRI data (Shin et al. 2014).

Resting-state functional connectivity (RSFC) analysis

Sub-regions of striatum were firstly defined based on the Harvard–Oxford Structural Atlas, a validated probabilistic atlas included in FSL. In this atlas, each voxel is assigned a value that corresponds to its probability of belonging to a given parceled region. In this study, we selected a 50% probability-weighted striatum atlas that included three sub-regions such as the bilateral caudate, putamen, and NAcc because the lateralization effects were not highlighted in previous studies. Seed-based resting-state functional connectivity maps were produced by extracting the BOLD time course from each seed region and then computing the correlational coefficients between that time course and the time courses from all other brain voxels. The correlational coefficients were converted to a normal distribution through Fisher's Z transform and then selected for further analyses, including the univariate and multivariate pattern analysis. In univariate analysis, group-level analyses were conducted by using a mixed-effects model (FLAME) implemented in FSL. Corrections for multiple comparisons were performed at the cluster level using Gaussian random field theory (voxel wise threshold $z > 3.1$ and cluster wise FWE corrected $p < 0.05$) (Eklund et al. 2016).

Support vector regression (SVR) analysis

The preprocessed RSFC data were employed to predict individual log$k$ using an Epsilon-insensitive support vector regression (SVR) (Drucker et al. 1997) with a linear kernel, as implemented in PyMVPA (Multivariate Pattern Analysis in Python; https://www.pymvpa.org/). A searchlight procedure with a three-voxel radius (Kriegeskorte et al. 2006) was utilized to produce the decoding accuracy in the neighborhood of each voxel. Following previous studies (Jimura and Poldrack 2012; Wang et al. 2016; He et al. 2013), we set the ε parameter in the SVR to be 0.01.

A ten-fold cross-validation was applied. The 429 participants were divided into 10 groups of 42 or 43 participants, with matched gender as well as matched log$k$, depending on the specific analysis. Firstly, age and gender were regressed out from RSFC of sub-regions of striatum and the residual were further subjected to SVR. Then, for each iteration, an SVR model was trained based on 386 or 387 participants. Once trained, this SVR model then generated a prediction from the score of the excluded 42 or 43 participants based on corresponded imaging data. Voxel-wise accuracy of SVR prediction was then calculated as the Pearson's correlation coefficient between actual and predicted values of the log$k$ and then transformed to the corresponding Z-score maps. To control the effect of head motion on RSFC, individuals' mean FDs were additionally regressed out and the residual were subjected to SVR in validation analysis. Multiple comparisons were corrected at the cluster level for each analysis (voxel wise threshold $z > 3.1$ and cluster wise FWE corrected $p < 0.05$)(Eklund et al. 2016).

Univariate correlation analysis

To further explore the direction of correlation between functional connectivity and behavioral delay-discounting rate (log*k*), we selected the significantly predicted multivariate brain region as the seed regions, and then extracted the average functional connectivity strength respectively with the subregions of striatum. Then, we calculated the correlational values between them and behavioral discounting rate (log*k*). Due to the double dipping problem, only relevant directions (i.e., positive or negative trend) but not the *r* and *p* value were further reported in our study.

Results

Behavioral results

The mean discounting rate (log*k*) assessed by the hyperbolic function was -1.96 ± 0.49 and its range was from -3.64 to -0.75. The mean FD was 0.11 ± 0.04 and its range was from 0.04 to 0.26. There was not a significant correlation between the log*k* and head motion ($r = -0.03$, $p = 0.61$), which suggests that head motion has a limited impact on consequent analysis. In addition, gender differences were also not observed in impulsivity ($t_{(427)} = 1.20$, $p = 0.231$).

RSFC network differences among the network of sub-regions of striatum

Figure 1 illustrates the functional networks of different striatum subdivisions and their network differences between them. In particular, significant functional connectivity with the NAcc seed regions was predominantly observed with the ventral medial prefrontal cortex (Fig. 1a) whereas significant functional connectivity with the caudate and putamen seeds regions was respectively found with the dorsal prefrontal cortex (Fig. 1b) and dorsal motor-related brain regions (Fig. 1c). In addition, stronger functional connectivity with the NAcc seed than the caudate seed was found in the ventral prefrontal cortex (vmPFC), posterior cingulate cortex (PCC), temporal lobe, hippocampus, and posterior occipital cortex (Fig. 1d, red areas) whereas stronger functional connectivity with the caudate seed than the NAcc was observed with the dorsal prefrontal cortex, SMG, mid-cingulate cortex, interior temporal cortex and insula (Fig. 1d, blue areas). Similarly, stronger functional connectivity with the NAcc seed than the putamen seed was found with the vmPFC, PCC, temporal pole, and hippocampus (Fig. 1e, red areas) whereas stronger functional connectivity with the putamen seed than the NAcc seed was observed in the dorsal prefrontal cortex, supplementary motor areas (SMA), precentral and postcentral gyrus, insula, and medial occipital cortex (Fig. 1e, blue areas). In contrast, stronger functional connectivity with the caudate seed than putamen seed was found in ventral and dorsal medial prefrontal cortex, PCC, interior temporal cortex, SMG, and frontal pole (Fig. 1f, red areas)

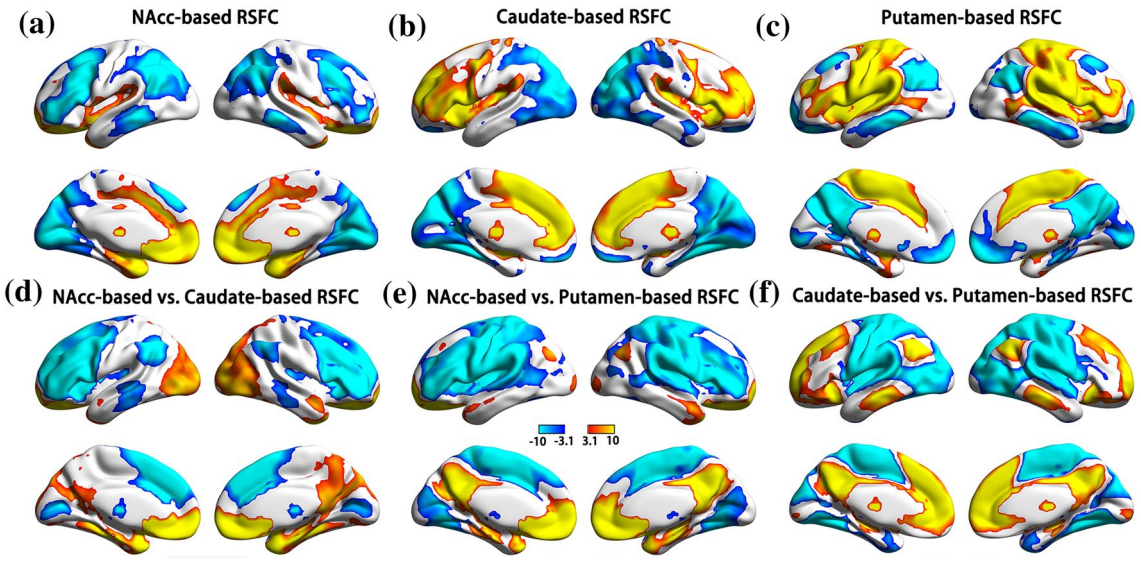

Fig. 1 Resting-state functional networks related to the NAcc-, caudate-, and putamen-seed regions and their functional network comparisons between them. (**a**–**c**), respectively, illustrates the functional networks of the striatum subdivisions. Red color indicates positive functional connectivity with the different seeds whereas blue indicates negative functional connectivity with different seeds. (**d**–**e**) Displays functional network comparisons between distinct seeds-based networks

whereas stronger functional connectivity with the putamen seed than the caudate seed was observed in the SMA, precentral and postcentral gyrus, and occipital cortex (Fig. 1f, blue areas). These findings suggest that striatum subdivisions respectively projected to distinct regions of prefrontal cortex, which may form distinct neural circuitries underlying different aspects of impulsivity.

NAcc-based RSFC's associations with delay-discounting rate

Firstly, we explored whether NAcc-based functional network predicts log*k* using MVPA. Our findings revealed that log*k* could be successfully predicted by the RSFC between the bilateral NAcc and limbic-prefrontal cortex, including the left medial orbitofrontal cortex extending to vmPFC (mOFC; peak point MNI = − 14, 30, − 24, *Z* = 4.01), right dorsolateral prefrontal gyrus (DLPFC; MNI = 26, 0, 64, *Z* = 3.29), and right frontal pole (FP; MNI = 24, 66, 0, *Z* = 4.05) (Fig. 2a). Other brain regions showing similar prediction accuracy included the left precuneus (MNI = − 6, − 46, 52, *Z* = 4.42), right lingual gyrus (MNI = 18, − 48, − 8, *Z* = 4.39), left central opercular cortex (MNI = − 54, − 14, 14, *Z* = 4.36), right frontal opercular cortex (MNI = 36, 18, 6, *Z* = 4.10), and right occipital pole (MNI = 18, − 100, 6, *Z* = 4.08) (Table 1). To probe the direction of the association between fronto-striatal RSFC and log*k*, further correlational analysis indicated that decision impulsivity (log*k*) was negatively correlated with the RSFC between the NAcc and DLPFC, but positively correlated with the RSFC between the NAcc and mOFC/VMPFC and FP (Fig. 2d).

Caudate-based RSFC's associations with delay-discounting rate

Using bilateral caudate as seed regions, we found that log*k* could be predicted by the RSFC between this seed region and the dorsal portions of the prefrontal cortex, including the right DMPFC (MNI = 12, 48, 24, *Z* = 4.41), right DLPFC (MNI = 18, 12, 66, *Z* = 3.76), and right middle frontal gyrus (MFG; MNI = 34, 12, 52, *Z* = 4.17)(Fig. 2b). Other brain regions showing similar prediction accuracy included the right supracalcarine (MNI = 16, − 64, 18, *Z* = 4.08), left postcentral (MNI = − 60, − 6, 24, *Z* = 5.02), right lateral occipital cortex (LOC; MNI = 48, − 78, 0, *Z* = 3.90), right supramarginal gyrus (SMG; MNI = 54, − 42, 20, *Z* = 3.72), and right Heschl's gyrus (MNI = 48, − 20, 12, *Z* = 5.26) (Table 1). Similarly, correlational analysis revealed that individual's decision impulsivity (log*k*) was positively correlated with all fronto-caudate coupling (Fig. 2e). Conjunction analysis revealed no common region between NAcc- and caudate-based RSFC associations with delay-discounting rate.

Putamen-based RSFC's associations with delay-discounting rate

Unlike our observations with the NAcc and caudate, log*k* was not predicted by the RSFC between the bilateral

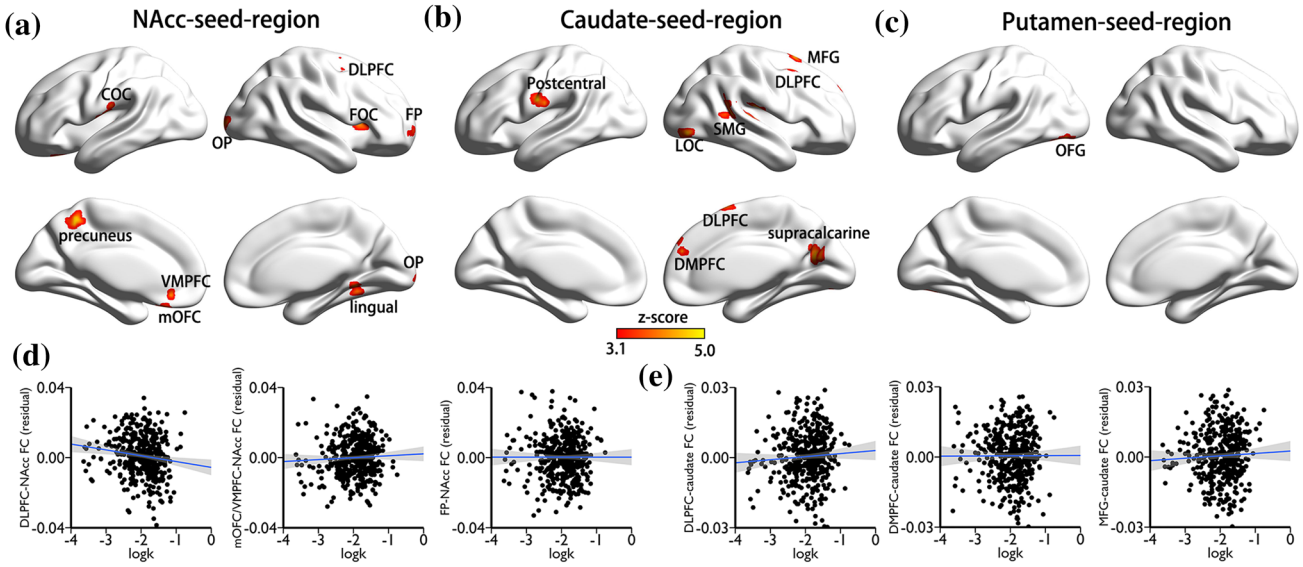

Fig. 2 MVPA and univariate results on the associations between dissociable fronto-striatal functional connectivities and delay discount rate (log*k*) after controlling for age and gender. (**a**–**c**) respectively illustrates the predictions of RSFC of the striatum subdivisions such as the NAcc, caudate, and putamen on individual's impulsivity. (**d**) and (**e**) exhibits the correlations between fronto-NAcc and fronto-caudate functional connectivity and log*k*

Table 1 Brain regions that RSFC of the striatum subdivisions predicted delay discounting rate in multivariate analysis after controlling for age and gender

Brain regions	L/R	No of voxels	MNI coordinates			*Z*
			x	*y*	*z*	
NAcc-Seed RSFC						
Medial OFC	L	86	− 14	30	− 24	4.01
SFG	R	85	26	0	64	3.29
Frontal pole	R	90	− 24	66	0	4.05
Frontal opercular cortex	R	124	36	18	6	4.10
Central opercular cortex	L	186	− 54	− 14	14	4.36
Precuneus	L	101	− 6	− 46	52	4.42
Lingual gyrus	R	108	18	− 48	− 8	4.39
Occipital pole	R	103	18	− 100	6	4.08
Caudate-seed RSFC						
DMPFC	R	175	12	48	24	4.41
SFG	R	137	18	12	66	3.76
Middle frontal cortex	R	133	34	12	52	4.17
Postcentral gyrus	L	138	− 60	− 6	24	5.02
SMG	R	112	54	− 42	20	3.72
LOC	R	115	48	− 78	0	3.90
Supracalcarine	R	142	16	− 64	18	4.08
Heschl's gyrus	R	175	48	− 20	12	5.26
Putamen-seed RSFC						
Occipital Fusiform gyrus	L	85	− 40	− 72	− 12	4.42

OFC orbitofrontal cortex, *SFG* superior frontal gyrus, *DMPFC* dorsomedial prefrontal cortex, *SMG* supramarginal gyrus, *LOC* lateral occipital cortex, *L* left, *R* right

putamen and the prefrontal cortex, though it was predicted by the RSFC between the bilateral putamen and the left occipital fusiform gyrus (MNI = − 40, − 72, − 12, Z = 4.42) (Table 1 and Fig. 2c). Conjunction analysis revealed no overlapping region between these three seed-based RSFC conditions.

When additionally controlling for head motion, the above-mentioned findings still remained significant (Figure S1 and Table S1). Therefore, these findings suggested that head motion did not influence the prediction of fronto-striatal RSFC upon choice impulsivity through the multivariate pattern analysis.

Discussion

This study used multivariate pattern analysis and a relatively large sample data to examine the extent to which fronto-striatal functional connectivity predicts choice impulsivity, assessed by the adaptive delay-discounting task. Our results indicated that the functional couplings between the NAcc and MPFC/DLPFC and between the caudate and DLPFC including DMPFC could successfully predict individual's delay-discounting rate (log$k$). However, such associations were not replicated for the functional connectivity between the putamen and prefrontal cortex. To the best of our knowledge, this is the first work to systematically and comprehensively delineate the contributions of distinct fronto-striatal functional couplings upon choice impulsivity combined with multivariate pattern analysis in a relatively large sample. These findings suggest that choice impulsivity may largely depend on dissociable fronto-striatal functional circuitries. This work further provides a better understanding of the importance of fronto-striatal circuitry on decision-making from the perspective of individual differences.

Ample imaging studies have especially emphasized the critical contributions of the valuation system including the NAcc, vmPFC, and mOFC on choice impulsivity (Peters and Büchel 2011; McClure et al. 2004). Such neural system's oversensitivity to immediate reward was associated with higher choice impulsivity, which has been considered as one of the potential neural substrates of choice impulsivity (McClure et al. 2004, 2007). Additionally, top-down cognitive control is able to modulate this system's activation in response to reward-related options to reduce choice impulsivity via biasing attention to delay option or weighting the future goals (McClure et al. 2004, 2007; Luo et al. 2009). In accordance with these findings, the functional coupling between the NAcc and mOFC/vmPFC and between the NAcc and DLPFC indeed predicted individual's choice impulsivity via a multivariate pattern analysis approach in present study. Such findings are also consistent

with previous studies that suggest associations between the fronto-striatal structural (Hampton et al. 2017; van den Bos et al. 2014, 2015), functional connectivity (Wang et al. 2016; Christakou et al. 2011), and the delay-discounting rate. Therefore, choice impulsivity might largely rely upon interactions within the valuation system and between the valuation system and cognitive control systems, through the different fronto-striatal connectivity patterns involved in these processes.

Dorsal striatum, mainly composing of the caudate and putamen, is involved in choice impulsivity and has been thought to associate with executive control (Eagle et al. 1999), cost overcoming (Benningfield et al. 2014), and decision value (Cai et al. 2011). Moreover, structural alteration in the dorsal striatum (i.e., caudate and putamen) was also correlated with choice impulsivity (Tschernegg et al. 2015). Interestingly, the functional connectivity between the caudate and DLPFC was found to be predictive of impulsive scores in present study. This is consistent with previous research that indicates the close associations between choice impulsivity and dorsal striatum-DLPFC white matter connectivity (Hampton et al. 2017). As such, we speculate that top-down cognitive control processes might down-regulate the value computation, executive function, and costs overcoming substrated by the caudate to reduce individual's impatience.

More interestingly, we observed that caudate-DMPFC functional connectivity could predict behavioral scores in choice impulsivity. The DMPFC is functionally thought to represent the subjective value of delayed rewards (Wang et al. 2014) and has been also implicated in high-level cognitive control processes (Ramnani and Owen 2004; Venkatraman et al. 2009) and exploratory decision (Daw et al. 2006), as well as is responsible for encoding information in relation to future, low certainty, or less tangibility (Bechara and Damasio 2005). In addition to the caudate's influence upon decision value, it may also be involved in choice impulsivity. That is, the subjective value of delayed options may be computed in the DMPFC and then subsequently compared by the caudate to make an adaptive decision. Such speculation still needs to call for empirical study to bridge the gap between theoretical hypothesis and experimental evidence via task-based fMRI design in future.

It should be noted, however, that in present study, we did not observe similar prediction patterns for putamen-prefrontal functional connectivity in choice impulsivity. Relative to the NAcc and caudate brain areas, the putamen is predominantly involved in motor execution (Morein-Zamir and Robbins 2015) and has functional connections with motor-related cortical regions such as premotor, supplementary motor areas (SMA), and preSMA (Di Martino et al. 2008). Importantly, our previous study has demonstrated the dissociated neural substrates between choice impulsivity and action impulsivity (Wang et al. 2016), which might imply that choice impulsivity does not rely on the putamen-prefrontal/motor cortices functional connectivity but still recruits the engagement of single brain region of putamen. In keeping with this speculation, some studies have likewise reported the associations of putamen functional activations and structural metrics in choice impulsivity (Tschernegg et al. 2015).

In this study, a multivariate pattern analysis approach and relatively large sample data were utilized to explore the underlying neural substrates of impulsive choice from the perspective of individual differences. Our findings not only promoted a deeper understanding of the neural basis of inter-temporal choice but also further emphasize the importance of dissociable fronto-striatal functional coupling patterns in inter-temporal choice. Although other studies have shown that striatal subdivision-related functional networks were inter-connected, we emphasized different nodes from a micro perspective. Additionally, it is necessary to further substantiate these findings in other independent samples and to implement clever experimental designs that can distinguish specific mental processes related to distinct fronto-striatal functional connectivities in impulsive choice. It is worth noting that 101 adolescents (age 17–18) were included in our analysis but no significant group differences between this group and adults group were observed in impulsivity scores ($t_{(427)} = 0.580$, $p = 0.494$) and in NAcc-/Caudate-based functional connectivity. Furthermore, adolescence period only altered the putamen-based functional coupling with VMPFC (MNI = − 3, 42, 0) but not the left occipital fusiform gyrus found in main analysis. Such findings hint that neurodevelopment changes from adolescence to adulthood may do not influence our key conclusion of different fronto-striatal loops supporting impulsivity. Additionally, this study is correlational in nature and cannot provide a causal description between fronto-striatal functional connectivity and impulsive choice. Finally, future work may wish to investigate white matter fiber fronto-striatal connections, to provide cross-validation and a more comprehensive perspective for human choice impulsivity.

In conclusion, our study showed dissociable fronto-striatal-dependent neural mechanisms of impulsivity and further provided a better understanding of the contributions of striatum subdivisions, as well as their functional connectivity with separate areas of prefrontal cortex, upon inter-temporal choice.

Funding This work was supported by research grants from the Humanities and Social Science Fund Project of the Ministry of Education (20YJC190018), National natural science foundation of China (31972906), open research fund of the key laboratory of mental health, Institute of Psychology, Chinese Academy of Sciences

(KLMH2019K05), and the High-end Foreign expert introduction program (G20190022029).

Data availability The data that support the findings of this study are available from the corresponding author upon reasonable request.

Compliance with Ethical Standards

Conflict of interest The authors declare that they have no conflict of interest.

Ethical approval All procedures performed in studies involving human participants were in accordance with the ethical standards of the institutional and national research committee and with 1964 Helsinki declaration and its later amendments or comparable ethical standards.

Informed consent Informed consent was obtained from all individual participants included in the study.

References

Alessi S, Petry NM (2003) Pathological gambling severity is associated with impulsivity in a delay discounting procedure. Behav Proc 64(3):345–354

Alexander GE, DeLong MR, Strick PL (1986) Parallel organization of functionally segregated circuits linking basal ganglia and cortex. Annu Rev Neurosci 9(1):357–381

Ballard K, Knutson B (2009) Dissociable neural representations of future reward magnitude and delay during temporal discounting. NeuroImage 45(1):143–150

Bari A, Robbins TW (2013) Inhibition and impulsivity: behavioral and neural basis of response control. Prog Neurobiol 108:44–79

Bechara A, Damasio AR (2005) The somatic marker hypothesis: a neural theory of economic decision. Games Econ Behav 52(2):336–372

Bechara A, Tranel D, Damasio H (2000) Characterization of the decision-making deficit of patients with ventromedial prefrontal cortex lesions. Brain 123(11):2189–2202

Benningfield MM, Blackford JU, Ellsworth ME, Samanez-Larkin GR, Martin PR, Cowan RL, Zald DH (2014) Caudate responses to reward anticipation associated with delay discounting behavior in healthy youth. Dev Cogn Neurosci 7:43–52

Bickel WK, Odum AL, Madden GJ (1999) Impulsivity and cigarette smoking: delay discounting in current, never, and ex-smokers. Psychopharmacol 146(4):447–454

Cai X, Kim S, Lee D (2011) Heterogeneous coding of temporally discounted values in the dorsal and ventral striatum during intertemporal choice. Neuron 69(1):170–182

Chib VS, Rangel A, Shimojo S, O'Doherty JP (2009) Evidence for a common representation of decision values for dissimilar goods in human ventromedial prefrontal cortex. J Neurosci 29(39):12315–12320

Christakou A, Brammer M, Rubia K (2011) Maturation of limbic corticostriatal activation and connectivity associated with developmental changes in temporal discounting. NeuroImage 54(2):1344–1354

Cooper N, Kable JW, Kim BK, Zauberman G (2013) Brain activity in valuation regions while thinking about the future predicts individual discount rates. J Neurosci 33(32):13150–13156

Dalley JW, Everitt BJ, Robbins TW (2011) Impulsivity, compulsivity, and top-down cognitive control. Neuron 69(4):680–694

Damoiseaux J, Rombouts S, Barkhof F, Scheltens P, Stam C, Smith SM, Beckmann C (2006) Consistent resting-state networks across healthy subjects. Proc Natl Acad Sci USA 103(37):13848–13853

Daw ND, O'doherty JP, Dayan P, Seymour B, Dolan RJ (2006) Cortical substrates for exploratory decisions in humans. Nature 441(7095):876

Dawe S, Gullo MJ, Loxton NJ (2004) Reward drive and rash impulsiveness as dimensions of impulsivity: implications for substance misuse. Addict Behav 29(7):1389–1405

Di Martino A, Scheres A, Margulies DS, Kelly A, Uddin LQ, Shehzad Z, Biswal B, Walters JR, Castellanos FX, Milham MP (2008) Functional connectivity of human striatum: a resting state FMRI study. Cereb Cortex 18(12):2735–2747

Drucker H, Burges CJ, Kaufman L, Smola AJ, Vapnik V Support vector regression machines. In: Advances in neural information processing systems, 1997. pp 155–161

Eagle DM, Humby T, Dunnett SB, Robbins TW (1999) Effects of regional striatal lesions on motor, motivational, and executive aspects of progressive-ratio performance in rats. Behav Neurosci 113(4):718

Eklund A, Nichols TE, Knutsson H (2016) Cluster failure why fMRI inferences for spatial extent have inflated false-positive rates. Proc Natl Acad Sci. https://doi.org/10.1073/pnas.1602413113

Figner B, Knoch D, Johnson EJ, Krosch AR, Lisanby SH, Fehr E, Weber EU (2010) Lateral prefrontal cortex and self-control in intertemporal choice. Nat Neurosci 13(5):538

Fox MD, Snyder AZ, Vincent JL, Corbetta M, Van Essen DC, Raichle ME (2005) The human brain is intrinsically organized into dynamic, anticorrelated functional networks. Proc Natl Acad Sci USA 102(27):9673–9678

Haber SN, Knutson B (2010) The reward circuit: linking primate anatomy and human imaging. Neuropsychopharmacology 35(1):4

Hampton WH, Alm KH, Venkatraman V, Nugiel T, Olson IR (2017) Dissociable frontostriatal white matter connectivity underlies reward and motor impulsivity. NeuroImage 150:336–343

Hare TA, Camerer CF, Rangel A (2009) Self-control in decision-making involves modulation of the vmPFC valuation system. Science 324(5927):646–648

Hare TA, Hakimi S, Rangel A (2014) Activity in dlPFC and its effective connectivity to vmPFC are associated with temporal discounting. Front Neurosci 8:50

Hariri AR, Brown SM, Williamson DE, Flory JD, de Wit H, Manuck SB (2006) Preference for immediate over delayed rewards is associated with magnitude of ventral striatal activity. J Neurosci 26(51):13213–13217

He Q, Xue G, Chen C, Chen C, Lu Z-L, Dong Q (2013) Decoding the neuroanatomical basis of reading ability: a multivoxel morphometric study. J Neurosci 33(31):12835–12843

Hu S, Ide JS, Zhang S, Sinha R, Chiang-shan RL (2015) Conflict anticipation in alcohol dependence—a model-based fMRI study of stop signal task. NeuroImage Clin 8:39–50

Jimura K, Poldrack RA (2012) Analyses of regional-average activation and multivoxel pattern information tell complementary stories. Neuropsychologia 50(4):544–552

Johnson MW, Bickel WK (2002) Within-subject comparison of real and hypothetical money rewards in delay discounting. J Exp Anal Behav 77(2):129–146

Kable JW, Glimcher PW (2007) The neural correlates of subjective value during intertemporal choice. Nat Neurosci 10(12):1625

Koritzky G, He Q, Xue G, Wong S, Xiao L, Bechara A (2013) Processing of time within the prefrontal cortex: recent time engages posterior areas whereas distant time engages anterior areas. NeuroImage 72:280–286

Kriegeskorte N, Goebel R, Bandettini P (2006) Information-based functional brain mapping. Proc Natl Acad Sci USA 103(10):3863–3868

Lagorio CH, Madden GJ (2005) Delay discounting of real and hypothetical rewards III: steady-state assessments, forced-choice trials, and all real rewards. Behav Proc 69(2):173–187

Li N, Ma N, Liu Y, He X-S, Sun D-L, Fu X-M, Zhang X, Han S, Zhang D-R (2013) Resting-state functional connectivity predicts impulsivity in economic decision-making. J Neurosci 33(11):4886–4895

Luo S, Ainslie G, Giragosian L, Monterosso JR (2009) Behavioral and neural evidence of incentive bias for immediate rewards relative to preference-matched delayed rewards. J Neurosci 29(47):14820–14827

Lv C, Wang Q, Chen C, Qiu J, Xue G, He Q (2019) The regional homogeneity patterns of the dorsal medial prefrontal cortex predict individual differences in decision impulsivity. NeuroImage 200:556–561

Lv C, Wang Q, Chen C, Xue G, He Q (2020) Activation patterns of the dorsal medial prefrontal cortex and frontal pole predict individual differences in decision impulsivity. Brain Imaging Behav. https://doi.org/10.1007/s11682-020-00270-1

McClure SM, Ericson KM, Laibson DI, Loewenstein G, Cohen JD (2007) Time discounting for primary rewards. J Neurosci 27(21):5796–5804

McClure SM, Laibson DI, Loewenstein G, Cohen JD (2004) Separate neural systems value immediate and delayed monetary rewards. Science 306(5695):503–507

Miller EK, Cohen JD (2001) An integrative theory of prefrontal cortex function. Annu Rev Neurosci 24(1):167–202

Mischel W, Shoda Y, Rodriguez MI (1989) Delay of gratification in children. Science 244(4907):933–938

Morein-Zamir S, Robbins TW (2015) Fronto-striatal circuits in response-inhibition: relevance to addiction. Brain Res 1628:117–129

O'Reilly RC (2010) The what and how of prefrontal cortical organization. Trends Neurosci 33(8):355–361

Paloyelis Y, Asherson P, Mehta MA, Faraone SV, Kuntsi J (2010) DAT1 and COMT effects on delay discounting and trait impulsivity in male adolescents with attention deficit/hyperactivity disorder and healthy controls. Neuropsychopharmacology 35(12):2414

Peper JS et al (2012) Delay discounting and frontostriatal fiber tracts: a combined DTI and MTR study on impulsive choices in healthy young adults. Cereb Cortex 23(7):1695–1702

Peters J, Büchel C (2011) The neural mechanisms of inter-temporal decision-making: understanding variability. Trends Cogn Sci 15(5):227–239

Ramnani N, Owen AM (2004) Anterior prefrontal cortex: insights into function from anatomy and neuroimaging. Nat Rev Neurosci 5(3):184

Ridderinkhof KR, Ullsperger M, Crone EA, Nieuwenhuis S (2004) The role of the medial frontal cortex in cognitive control. Science 306(5695):443–447

Shin D-J, Jung WH, He Y, Wang J, Shim G, Byun MS, Jang JH, Kim SN, Lee TY, Park HY (2014) The effects of pharmacological treatment on functional brain connectome in obsessive-compulsive disorder. Biol Psychiatry 75(8):606–614

Tschernegg M, Pletzer B, Schwartenbeck P, Ludersdorfer P, Hoffmann U, Kronbichler M (2015) Impulsivity relates to striatal gray matter volumes in humans: evidence from a delay discounting paradigm. Front Hum Neurosci 9:384

van den Bos W, Rodriguez CA, Schweitzer JB, McClure SM (2014) Connectivity strength of dissociable striatal tracts predict individual differences in temporal discounting. J Neurosci 34(31):10298–10310

Van Den Bos W, Rodriguez CA, Schweitzer JB, McClure SM (2015) Adolescent impatience decreases with increased frontostriatal connectivity. Proc Natl Acad Sci. https://doi.org/10.1073/pnas.1423095112

Venkatraman V, Rosati AG, Taren AA, Huettel SA (2009) Resolving response, decision, and strategic control: evidence for a functional topography in dorsomedial prefrontal cortex. J Neurosci 29(42):13158–13164

Wang Q, Chen C, Cai Y, Li S, Zhao X, Zheng L, Zhang H, Liu J, Chen C, Xue G (2016) Dissociated neural substrates underlying impulsive choice and impulsive action. NeuroImage 134:540–549

Wang Q, Luo S, Monterosso J, Zhang J, Fang X, Dong Q, Xue G (2014) Distributed value representation in the medial prefrontal cortex during intertemporal choices. J Neurosci 34(22):7522–7530

Wittmann M, Leland DS, Paulus MP (2007) Time and decision making: differential contribution of the posterior insular cortex and the striatum during a delay discounting task. Exp Brain Res 179(4):643–653

Xu L, Liang Z-Y, Wang K, Li S, Jiang T (2009) Neural mechanism of intertemporal choice: from discounting future gains to future losses. Brain Res 1261:65–74